JOURNAL OF GUIDANCE, CONTROL, AND DYNAMICS
Vol. 26, No. 4, July–August 2003

Automated Method to Compute Orbital Reentry Trajectories with Heating Constraints

Curtis Zimmerman,* Greg Dukeman,† and John Hanson‡
NASA Marshall Space Flight Center, Huntsville, Alabama 35812

An algorithm is presented that is designed to compute reentry trajectories for unpowered lifting reusable launch vehicles. The algorithm uses self-contained trajectory simulation and root finding techniques to determine the appropriate control sequences for solving reentry problems. For orbital reentries, the solution process breaks the trajectory into two distinct parts. The first part begins where the deorbited vehicle first encounters substantial atmosphere and can exercise trajectory control through the manipulation of aerodynamic lift. This phase of the flight is governed by an analytical, constant heat-rate following, bank angle control law. The second and final part of the trajectory begins where heat-rate control is no longer desired. During this time trajectory control is used to meet terminal range and altitude targets and is governed by a linear bank angle control law. The planning algorithm determines the value of the individual trajectory control parameters that shape the reentry. The planned trajectory is then used by a profile following guidance algorithm during actual flight. Test results for a variety of orbital and suborbital missions are shown.

Downloaded by UNIVERSITY OF OKLAHOMA on January 28, 2015 | http://arc.aiaa.org | DOI: 10.2514/2.5096

Nomenclature

C_D	=	drag coefficient
C_L	=	lift coefficient
D	=	drag acceleration
$\bar{g}$	=	gravitational acceleration
h	=	altitude
L	=	lift acceleration
m	=	mass
$\dot{Q}$	=	heat rate
r	=	radial distance from the center of the Earth to the vehicle
$\boldsymbol{r}_{\text{term}}$	=	inertial position vector at EGuide simulation termination point
$\boldsymbol{r}_{\text{HAC}}$	=	inertial position vector of heating alignment cone target
S_{ref}	=	reference area
t_{current}	=	current time in EGuide simulation
t_{init}	=	initial time in EGuide simulation
V	=	Earth-relative velocity magnitude of the vehicle
γ	=	relative flight path angle
ζ	=	damping ratio
θ	=	longitude
μ	=	gravitational constant
ρ	=	atmospheric density
σ	=	bank angle
σ_i	=	bank angle initialization parameter
σ_{slope}	=	bank angle slope parameter
φ	=	azimuth of V measured clockwise from north
ϕ	=	latitude
ω	=	rotation rate of the Earth
ω_n	=	time constant

Presented as Paper 2002-4454 at the AIAA Guidance, Navigation and Control Conference, Monterey, CA, August 2002; received 28 October 2002; revision received 28 March 2003; accepted for publication 31 March 2003. This material is declared a work of the U.S. Government and is not subject to copyright protection in the United States. Copies of this paper may be made for personal or internal use, on condition that the copier pay the $10.00 per-copy fee to the Copyright Clearance Center, Inc., 222 Rosewood Drive, Danvers, MA 01923; include the code 0731-5090/03 $10.00 in correspondence with the CCC.

*Aerospace Engineer, Guidance, Navigation, and Control Group.
†Guidance and Navigation Specialist, Guidance, Navigation, and Control Group.
‡Team Lead, Guidance, Navigation, and Control Group.

Introduction

IN the design of reentry trajectories for reusable launch vehicles (RLVs), two control variables are normally available: α (angle of attack) and σ (bank angle).[1] The entry guidance (EGuide) algorithm developed in this paper primarily attempts to find and adjust bank angle profiles to meet terminal conditions while maintaining a constant or predetermined angle-of-attack profile. The key feature that makes EGuide different from traditional guidance methods is its ability to solve trajectory problems onboard. Although research into entry guidance algorithms with numerical solution capability is not new,[2–4] their use as actual flight software remains untapped. This is due mainly to issues of computational complexity that accompany all numerical procedures of this nature. Previous work in this area has explored the predictor–corrector style of guidance algorithm. Predictor–corrector methods determine onboard, during flight, a trajectory control sequence that will transport the vehicle from its current state to a specified target. The solution process is repeated throughout the flight to correct for errors and dispersions. Simplicity is key. Even with the blazing speed of modern digital computers, it is important to make the trajectory problem solvable.

Recently, there has been interest in an algorithm architecture that combines the onboard solution capability of a predictor–corrector with traditional profile following entry guidance methods. The so-called planner/follower guidance uses an onboard solver in a trajectory planning stage that is executed sometime before the entry guidance cycle. The planner, behaving like a single execution of a predictor–corrector, determines the trajectory control sequence that will safely transport the vehicle from its initial state to a specified target. The follower then takes the trajectory control solution generated by the planner and uses it as a reference profile. The planner/follower shares with the predictor–corrector the ultimate need to make the trajectory problem solvable. However, unlike the predictor–corrector algorithm, the solution process (and the possibility of its heavy computational load) exists outside of the guidance cycle. Mease et al. have applied this strategy in the development of a method based on the drag planning technique used in space shuttle entry guidance.[5] Their planner, which considers both the longitudinal and the lateral motion of the entry trajectory, can use both angle-of-attack and bank angle control to arrive at a solution and is designed to satisfy path constraints along the way. Shen and Lu have developed a planner that makes use of the quasi-equilibrium glide condition to satisfy path constraints.[6] Their process of solution, which breaks the entry problem into two sequential one-parameter search problems, is designed to be simple and fast. Roenneke's planning method performs an onboard trajectory optimization with the objective of maximizing the vehicle's ranging authority.[7] His process uses an analytical

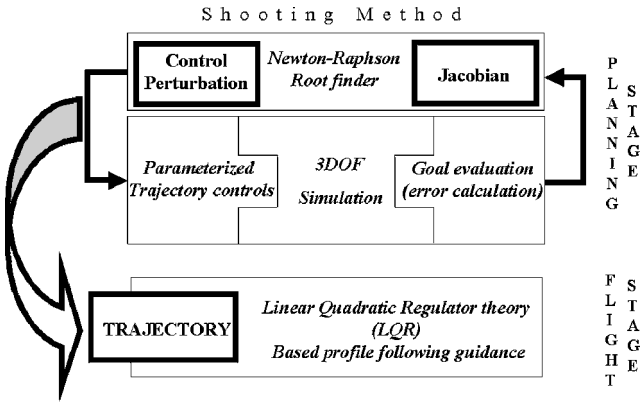

Fig. 1 Planner/follower entry guidance methodology.

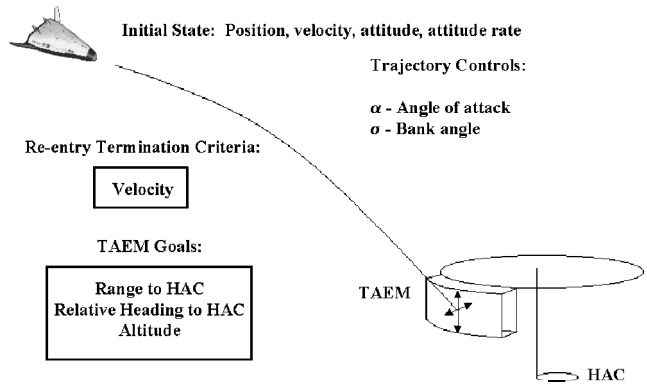

Fig. 2 Terminal conditions for reentry trajectories.

ranging problem so that each iteration of the optimization produces a feasible trajectory.

The EGuide planner, described in this paper, breaks an orbital entry problem into two distinct phases. The first phase is governed by an analytical heat-rate tracking bank angle control law and is characterized by a smooth altitude profile and a constant vehicle heat rate. The second phase is governed by a linear bank angle control law and is used to target the desired terminal conditions of the vehicle. The solution process adjusts parameters in each of these phases to arrive at the final orbital entry trajectory. A classical shooting method is used. The solution derived onboard by the EGuide planner supplies trajectory information to Dukeman's linear quadratic regulator (LQR)[8] profile following entry guidance algorithm for the actual flight (Fig. 1). Development and testing of EGuide has been carried out using the MAVERIC simulation. MAVERIC is a full six-degree-of-freedom (6-DOF) simulation developed to test guidance and control algorithms for the X-33 suborbital technology demonstration vehicle.

Shooting Method

EGuide solves the two-point boundary value problem of a reentry trajectory using mnewt,[9] a multidimensional Newton–Raphson root finding algorithm. The mnewt Jacobian matrix is generated by measuring the effect of trajectory control changes on the final state of simulated flights. EGuide uses a self-contained 3-DOF trajectory simulation (independent from MAVERIC) that models motion over a rotating oblate Earth with a United States Standard Atmosphere 1962. The equations of motion are integrated using a Fourth-order Runge–Kutta algorithm with a fixed step size of 1 s.

Initial Conditions

The goal of the EGuide planner is to provide safe reentry trajectory solutions for un-powered lifting RLVs. It is important for the planner to find solutions to the reentry problem (assuming they exist) from the entire range of initial conditions that may arise during an RLV mission. Therefore, in addition to computing reentry trajectories for vehicles returning from low Earth orbit, the planner must also be capable of determining safe trajectories for a wide variety of suborbital conditions. Suborbital reentry trajectories, which may be part of a specific mission design, are also commonly associated with abort situations that occur during ascent to orbit. Initiation of a suborbital reentry trajectory following an ascent occurs shortly after main engine cutoff (MECO) once the vehicle is on a descending flight path.

For a vehicle returning to Earth from orbit, a significant portion of the trajectory following the deorbit burn is spent outside of the region where aerodynamic trajectory control is possible. For this reason, the actual trajectory that is planned by EGuide and governed by reentry guidance does not begin until the vehicle encounters enough atmosphere to allow active trajectory control through manipulation of the lift vector. Initial conditions of the reentry state used by the EGuide planner are provided by a navigation subsystem and consist of position, velocity, attitude, and attitude rate measurements of the vehicle.

Terminal Conditions

Termination of all reentry trajectories (orbital and suborbital, simulated and real) occurs at a specified velocity. For the trajectory to be considered feasible, the termination point must be within the bounds of a "box" specified by altitude, range, and heading measured relative to a fixed ground-based latitude/longitude target (Fig. 2). The latitude/longitude target is a tangency point on an imaginary object referred to as the heading alignment cone (HAC), which is located near the end of a runway.

Immediately following reentry, the guidance responsibility for the vehicle is transferred to a terminal area energy management (TAEM) guidance system. Thus, the terminal target conditions or TAEM box conditions are specified in the following manner: 1) range to HAC at TAEM, 2) relative heading to HAC at TAEM, and 3) altitude at TAEM. The location of the HAC latitude/longitude target is defined before operation of the EGuide planner. The relative placement and bounds of the TAEM box is a specification given by the individual RLV.

Suborbital Reentry Planning

Part of EGuide is dedicated to solving the two-point boundary value problem of a suborbital reentry trajectory. Specifically, it tries to figure out how to deliver a vehicle from a variety of widely dispersed suborbital reentry conditions to a point within the bounds of a TAEM box. To solve the suborbital problem, a classical shooting method is used. Trajectory simulations are begun at a fixed initial suborbital state and are terminated at a specified velocity. Angle of attack and bank angle are used for trajectory control. The angle-of-attack profile for the flight is predefined as a function of Mach number. A linear equation is used to define the bank angle. At each time point during an EGuide trajectory simulation, the bank angle is computed using the following formulation:

$$\sigma = \mathrm{abs}[\sigma_{\mathrm{slope}} + \sigma_i(t_{\mathrm{current}} - t_{\mathrm{init}})] \tag{1}$$

The relative heading to HAC is maintained within a specified corridor during a simulated flight through the use of periodic bank sign reversals that are allowed to execute instantaneously (zero maneuver time). This forces the velocity heading of the vehicle to stay pointed at the HAC target. In the event that the simulated trajectory has too much range and overflies the HAC, velocity heading control acts so that the vehicle maintains a straight flight within the same corridor limits. On termination of a simulated trajectory, range and altitude performance is measured, and an end state error vector is computed. Because in the planning simulations the vehicle is always flying directly toward or away from the HAC target, a simple distance formula can be used to determine the range to HAC at the simulation termination point:

$$\text{range to HAC} = \cos^{-1}[\boldsymbol{r}_{\mathrm{term}}/|\boldsymbol{r}_{\mathrm{term}}| \cdot \boldsymbol{r}_{\mathrm{HAC}}/|\boldsymbol{r}_{\mathrm{HAC}}|] \cdot |\boldsymbol{r}_{\mathrm{HAC}}| \tag{2}$$

Downloaded by UNIVERSITY OF OKLAHOMA on January 28, 2015 | http://arc.aiaa.org | DOI: 10.2514/2.5096

Downloaded by UNIVERSITY OF OKLAHOMA on January 28, 2015 | http://arc.aiaa.org | DOI: 10.2514/2.5096

Range and altitude errors at the trajectory termination point are computed by comparison with the requirements of the TAEM box. The shooting method process of solution starts with the flight of a simulated trajectory using an initial guess for the variable bank angle control parameters σ_i and σ_{slope}. The altitude and range errors for this nominal trajectory are recorded. Then σ_i and σ_{slope} are each separately perturbed from their original values (one at a time) by a specified amount, and a simulated trajectory is flown for each perturbation to measure the effect on altitude and range error. The altitude and range error information from the nominal and perturbed simulated trajectories in conjunction with knowledge of the amount of perturbation applied to each control parameter is sufficient to provide a set of two simultaneous equations with two unknowns:

$$\begin{bmatrix} \dfrac{\delta\text{altitude}_{\text{error}}}{\delta\sigma_i} & \dfrac{\delta\text{altitude}_{\text{error}}}{\delta\sigma_{\text{slope}}} \\ \dfrac{\delta\text{range}_{\text{error}}}{\delta\sigma_i} & \dfrac{\delta\text{range}_{\text{error}}}{\delta\sigma_{\text{slope}}} \end{bmatrix} \begin{bmatrix} \Delta\sigma_i \\ \Delta\sigma_{\text{slope}} \end{bmatrix} = \begin{bmatrix} -\text{altitude}_{\text{error}} \\ -\text{range}_{\text{error}} \end{bmatrix} \tag{3}$$

Equation (3) is solved using the multidimensional root solver mnewt. The solution of Eq. (3) produces an updated nominal value for the bank angle control parameters σ_i and σ_{slope}. One iteration of the shooting process for the two free parameters requires three trajectory simulations. Convergence occurs when the range and altitude errors of a nominal trajectory simulation are within the bounds of the TAEM box.

Constant Heat-Rate Tracking

Although Eq. (1) can be used to generate valid trajectories from orbital reentry states, it does not contain enough flexibility to consistently return practical solutions. Heat and dynamic pressure constraints must somehow be addressed to assure safe flight conditions. Heating in particular can be effectively controlled using a bank angle formulation designed to maintain a constant heat rate during flight in the relevant portion of atmospheric entry.

Equations of Motion

From the 3-DOF equations of motion for a vehicle flying over a spherical rotating Earth, we have[10]

$$\dot{r} = V \sin\gamma$$

$$\dot{V} = -D - (\mu/r^2)\sin\gamma$$

$$\dot{\gamma} = (1/V)\{L\cos\sigma + [V^2 - (\mu/r)](\cos\gamma/r) + 2\omega V\cos\varphi\cos\phi\} \tag{4}$$

where L and D are aerodynamic lift and drag accelerations and are given by $L = 1/2m\rho V^2 S_{\text{ref}} C_L$ and $D = 1/2m\rho V^2 S_{\text{ref}} C_D$. The atmospheric density ρ is approximated by the exponential expression $\rho = \rho_0 e^{-\beta h}$, where ρ_0 and β are constants.

Heat-Rate Control

For a vehicle entering a planetary atmosphere, the time rate of average heat input per unit area can be estimated with the expression[11]

$$\dot{Q} = C\sqrt{\rho}V^n \tag{5}$$

where $n = 3.15$ and C is a constant. Heat-rate tracking guidance begins with the definition of an error term,

$$e = \dot{Q} - \dot{Q}_{\text{ref}} \tag{6}$$

The intent is for the error term to exhibit the behavior of a stable second-order feedback system. To accomplish this, it is substituted into the following classical second-order system:

$$\ddot{e} + 2\zeta\omega_n\dot{e} + \omega_n^2 e = 0 \tag{7}$$

The three preceding equations along with the equations of motion yield the following bank angle formulation:

$$\sigma = \cos^{-1}\left\{\frac{(\dot{\gamma} - V/r + \bar{g}/v)(V/D)}{(L/D)_{\text{est}}}\right\} \tag{8}$$

$$\dot{\gamma} = \frac{-a - 2\zeta\omega_n\ddot{Q} - \omega_n^2(\dot{Q} - \dot{Q}_{\text{ref}})}{b} \tag{9}$$

where a and b are expressions derived from a simplified format of the second time derivative of Eq. (5),

$$\ddot{Q} = a + b\dot{\gamma} \tag{10}$$

Thus, given a reference heat rate $\dot{Q}_{\text{ref}}$ and with use of Eq. (8) to generate bank angle control commands, the vehicle is expected to track a constant heat rate.

Orbital Reentry Planning

The initiation of reentry guidance in a return from low Earth orbit occurs once the vehicle encounters dense enough atmosphere to generate aerodynamic lift. The heating environment is an immediate concern because in this early portion of the reentry the speed of the vehicle is still close to orbital velocity. The EGuide planning simulation is configured to formulate trajectories that start with constant heat-rate tracking. The heat-rate tracking parameter $\dot{Q}_{\text{ref}}$, whose value determines what constant heat the vehicle will follow, can be used to shape the overall trajectory. Figure 3 shows the effect of variation of Q_{ref} on orbital reentry trajectories. Given the same set of orbital re-entry initial conditions, lower values of $\dot{Q}_{\text{ref}}$ produce trajectories that descend into the atmosphere more slowly and have more range than higher values of $\dot{Q}_{\text{ref}}$. However, the heat-rate tracking parameter alone is not sufficient to target all of the desired terminal conditions of the reentry problem. Additionally, heat-rate tracking is generally not an effective control in the latter portion of an orbital reentry when high heating is no longer present. For these reasons, terminal targeting is accomplished with the earlier described suborbital guidance. The orbital reentry trajectory is fully characterized by four parameters (Fig. 4). The first

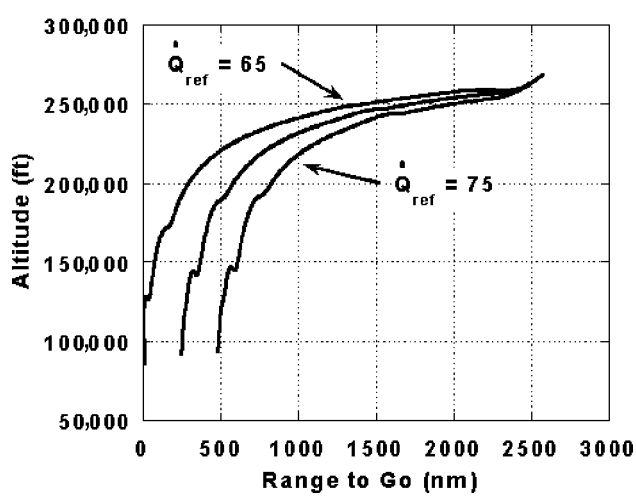

Fig. 3 Altitude vs range for three values of $\dot{Q}_{\text{ref}}$.

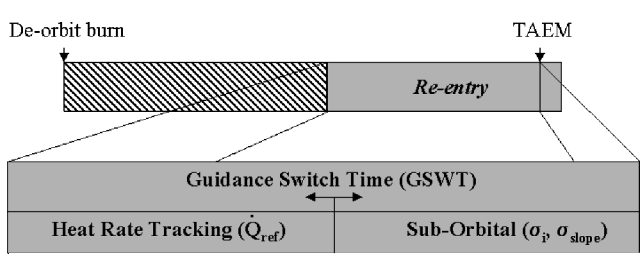

Fig. 4 Four parameters of an EGuide orbital reentry trajectory.

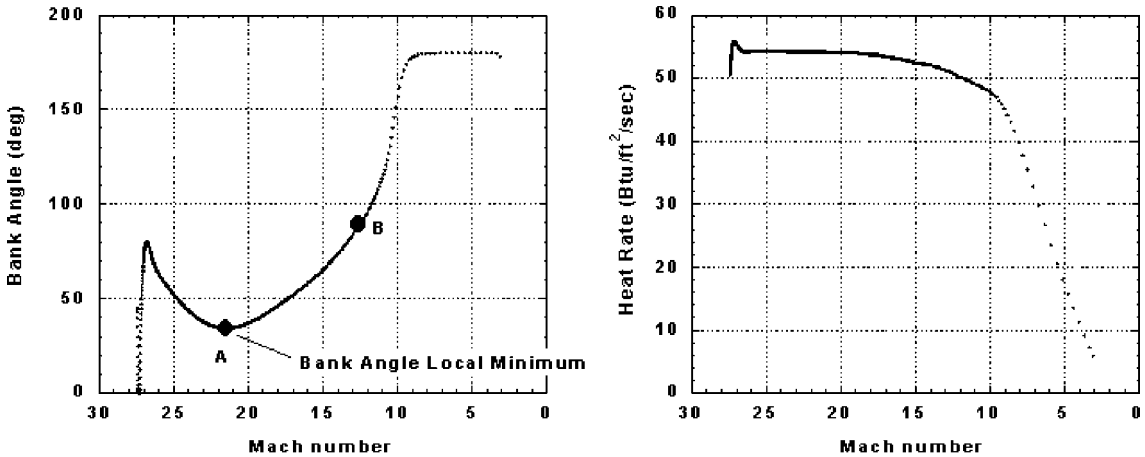

a) Bank angle vs Mach b) Heat rate vs Mach

Fig. 5 Heat-rate tracking bank angle profile with the corresponding heat-rate profile.

three parameters, $\dot{Q}_{\text{ref}}$, σ_i, and σ_{slope}, are from the heat-rate tracking and suborbital guidance formulations. The fourth parameter is the time chosen to terminate heat-rate tracking and switch to suborbital guidance and is referred to as the guidance switch time (GSWT).

Finding the GSWT

Calculation of the GSWT parameter is based on observed bank angle behavior during a simulated orbital reentry using heat-rate tracking. As shown in Fig. 5, in the very first part of an orbital reentry, heat-rate tracking guidance may modulate the bank angle quickly as the control "latches on" to the specified reference heat rate. This initial transient behavior gives way to a slower varying bank angle, which is decreasing in magnitude as the control tracks the reference. If heat-rate tracking is allowed to remain active indefinitely, the magnitude of the bank angle eventually begins to increase and finally becomes excessive as the control struggles to track a reference heat rate it can no longer sustain. The main feature of interest in the bank angle vs Mach plot of Fig. 5 is the local minimum that occurs at approximately Mach 21.5 (point A). Point A is designated as the GSWT. In actuality, good solutions to the orbital re-entry problem may exist by switching guidance formulations anywhere along the bank angle profile between points A and B. However, point A offers the advantage of being an event that is easily detectable. EGuide is programmed to find point A by simulating an orbital reentry (using heat-rate tracking guidance exclusively) and looking for the last occurrence of a bank angle minimum. The fact that the bank angle magnitude must increase after point A to maintain the reference heat rate indicates that the high heating portion of the flight has passed.

Setting the Reference Heat-Rate Parameter

The reference heat-rate parameter $\dot{Q}_{\text{ref}}$ can be thought of as the independent variable of an EGuide orbital reentry problem. The three other variable parameters, GSWT, σ_i, and σ_{slope}, are all essentially dependant on the selection of $\dot{Q}_{\text{ref}}$. Solving the orbital reentry problem boils down to identifying an appropriate reference heat-rate value that will (in combination with the three remaining variable parameters) result in acceptable behavior for the duration of the trajectory. The search for $\dot{Q}_{\text{ref}}$ is bounded. The lower bound is found by observing what reference heat-rate, when tracked for the duration of a simulated flight, results in the least range error from the TAEM target at the GSWT. The upper bound can be set from actual vehicle heat-rate constraints, although it may be possible to simulate a successful orbital reentry trajectory at a higher heat-rate than the vehicle can withstand. With upper and lower bounds set for the reference heat-rate parameter, EGuide can begin the search for the solution to the orbital reentry problem. When began with $\dot{Q}_{\text{ref}}$ at its lower bound, a three step iterative process is used.

1) Compute the GSWT based on the reference heat rate.

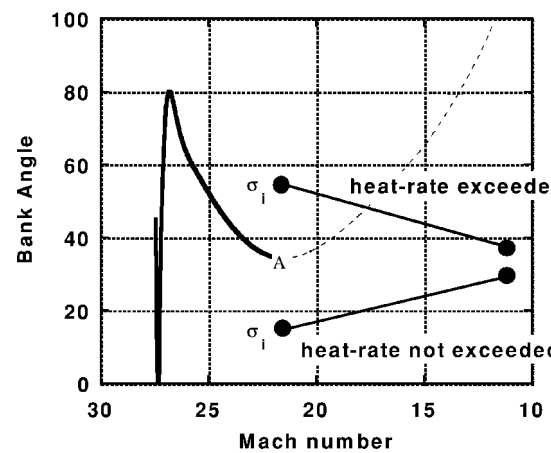

Fig. 6 Evaluation of the suborbital guidance solution.

2) Using the suborbital guidance formulation, solve the two-point boundary value problem that starts at the GSWT (point A) and ends at TAEM.

3) Evaluate the solution: If any part of the line segment defined by the suborbital guidance parameters σ_i and σ_{slope} is above the constant heat-rate curve, the chosen reference heat-rate will be exceeded during the suborbital guidance portion of the flight (Fig. 6). This is an indication that the reference heat rate is set too low. EGuide performs a limited version of this test by comparing the value of σ_i with the local minimum of the bank angle at point A. If σ_i is greater than the bank angle value at point A, the reference heat rate is increased by one unit, and the process is repeated starting at step 1. Convergence of the process occurs when σ_i is less than or equal to the local minimum of the bank angle at point A or, in other words, when the reference heat rate is not exceeded during suborbital guidance.

Flight Guidance

Once the planner has converged to a good solution, the trajectory information is used as a reference to fly the vehicle from the initial reentry state to TAEM. For orbital reentries, EGuide uses the computed value of $\dot{Q}_{\text{ref}}$ as a reference to fly a constant heat-rate profile (using the constant heat-rate tracking guidance) rather than handing off the responsibility to the LQR profile following flight guidance. The main advantage of this strategy is the direct influence over heat rate through feedback control. At the GSWT, EGuide acts as a predictor-corrector by performing a single update to the suborbital guidance parameters before recording the final trajectory and handing off the results to be flown by the LQR guidance. The LQR reference profile consists of altitude, range-to-go, and flight-path

Downloaded by UNIVERSITY OF OKLAHOMA on January 28, 2015 | http://arc.aiaa.org | DOI: 10.2514/2.5096

Downloaded by UNIVERSITY OF OKLAHOMA on January 28, 2015 | http://arc.aiaa.org | DOI: 10.2514/2.5096

angle states vs energy and bank angle and angle-of-attack controls vs energy.

Operational Notes

The EGuide planning process requires the input of an initial reentry state, a vehicle aerodynamic model, and specification of the required terminal conditions (TAEM and HAC). No other information or mission-dependant tuning is required. Figure 7 shows possible operational execution strategies for using EGuide as an onboard planner. For suborbital flight, EGuide may be executed immediately following MECO before the vehicle actually begins its reentry. For computing return trajectories from low Earth orbit, it is feasible that the planning process could take place even before the deorbit burn. In both cases, calculation of the reentry trajectory takes place outside of the actual guidance cycle. Once reentry begins, profile following methods are used to provide reliable performance during the guidance cycle.

Test Results

Vehicle Model

The X-33, a half-scale suborbital test vehicle designed for demonstration of single-stage-to-orbit technologies, was used for all testing of EGuide. The X-33 incorporates a number of unique features, including a linear aerospike main propulsion system, structurally integrated fuel and oxidizer tanks, and a metallic thermal protection system. The vehicle is a lifting-body configuration with an L/D of about 1.1 during hypersonic flight and has an approximate dry weight of 38,000 kg. Although the actual X-33 was strictly limited to suborbital flight, the vehicle model is used in tests for a variety of missions returning from low Earth orbit.

Terminal Conditions

Termination of the reentry trajectory occurs at a velocity of 3000 ft/s (914.4 m/s). At the trajectory termination point, the vehicle is required to be within a specified range, heading, and altitude with respect to a HAC latitude/longitude target. For the X-33, terminal target conditions for re-entry are as follows: 1) range to HAC = 30 nm ± 6 nm, 2) relative heading to HAC = 0 deg ± 10 deg, and 3) altitude = 96,000 ft ± 6000 ft.

Suborbital Reentry Results

Two missions are used for suborbital guidance algorithm testing. The first mission (X-33-1) represents a nominal trajectory, whereas the second (X-33-2) uses a higher energy trajectory. Both missions launch from Edwards Air Force Base, California, and land at Michael Army Airfield, Dugway Proving Ground, Utah. Undispersed initial reentry conditions for the missions are shown in Table 1. Dispersion analysis was performed using Monte Carlo simulations run on the MAVERIC simulation platform. Dispersions of the suborbital simulations (which start at launch) include variables relating to engine performance during ascent (thrust, mixture ratio, etc.), aerodynamic uncertainty, navigation accuracy, and vehicle mass properties, as well as atmospheric density and wind variations generated through the use of the Global Reference Atmospheric Model (GRAM).[12] Results of 100 simulated flights of each suborbital mission are shown in Table 2. In addition to the nominal missions, flights with exceptional circumstances are also included. Large thrust dispersions during ascent simulate mismodeled engine performance. Power pack out (PPO) cases simulate losing 50% of nominal engine thrust at various times during ascent. Results for these flights are shown in Table 3.

Table 1 Initial states for two suborbital reentry missions

	State					
Missions	h, ft	θ, deg	ϕ, deg	V, ft/s	γ, deg	ψ, deg
X-33-1	183,041	−116.19	36.57	9248	0.74	34.82
X-33-2	178,105	−114.88	37.97	8559	−2.26	36.74

Orbital Reentry Results

Results from six orbital re-entry missions flown with the X-33 vehicle are shown. Missions 1–3 represent three return opportunities from a 248-n mile circular orbit with inclination of 51.6 deg. The peak heat objective for missions 1–3 is 75 Btu · ft^2/s. Missions 4–6 represent three return opportunities from a 150-n mile circular orbit with inclination of 28.5 deg. The peak heat objective for missions 4–6 is 60 Btu · ft^2/s. All missions land at the Kennedy Space Center (KSC). Ground track and altitude profiles for the nominal missions are shown in Figs. 8 and 9. A representative bank angle and heat rate profile generated by EGuide for mission 1 is shown in Fig. 10 and 11. Note from Fig. 10 that the planner makes frequent bank reversals near the end of the trajectory compared to the actual flight guidance. This is because the EGuide planner and the LQR follower have independent bank reversal strategies. The planner, which is allowed to make instantaneous maneuvers, stays pointed at the HAC. An alternate strategy would be to use the planner to design a trajectory with a single bank reversal.

Dispersion analysis was performed on the orbital missions using Monte Carlo simulations. Dispersion quantities include variables relating to aerodynamic uncertainty, navigation accuracy, and vehicle mass properties, as well as variations in atmospheric density and winds generated by GRAM. The missions were run by initializing the MAVERIC simulation at a reentry state starting from approximately 400,000 ft. The initialization state of the MAVERIC simulation for each of the missions was undispersed. The actual reentry initial conditions provided to the EGuide planner (shown in Table 4) were dispersed by the cited uncertainties in the coast from the 400,000-ft starting point to the entry guidance interface point. Results for each of the missions are shown in Tables 5 and 6.

Table 3 Results for 3-DOF X-33-1 mission off-nominal cases

Mission	Range, nm	Altitude, ft	Heading, deg	Iterations
40-s PPO	26.92	100,179	−0.50	4
50-s PPO	29.75	95,764	6.25	3
60-s PPO	29.95	96,657	0.61	3
112-s PPO	28.27	97,209	2.93	4
+4 Sigma thrust	25.82	97,552	6.69	4
+6 Sigma thrust	26.22	97,620	8.74	4

Table 4 Initial states for six orbital reentry missions

	State					
Missions	h, ft	θ, deg	ϕ, deg	V, ft/s	γ, deg	ψ, deg
1	269,188	−107.43	−5.73	24,970	−0.79	35.8
2	269,215	−100.89	−10.00	24,974	−0.78	36.33
3	269,180	−115.83	0.36	24,961	−0.78	35.85
4	269,318	−114.24	−14.91	24,910	−0.39	37.29
5	269,312	−107.89	−18.60	24,909	−0.46	38.33
6	269,115	−122.60	−9.16	24,901	−0.40	36.60

Table 2 Results of 6-DOF Monte Carlo simulations, 100 runs each

	Mission X-33-1		Mission X-33-2	
Parameter	Average	Standard deviation	Average	Standard deviation
Range to HAC, n mile	30.24	1.14	30.86	0.56
Relative heading to HAC, deg	3.72	1.70	2.27	2.30
Altitude, ft	95,837	943	98,099	1878
Planner iterations	2.8	0.42	4.47	1.87

Downloaded by UNIVERSITY OF OKLAHOMA on January 28, 2015 | http://arc.aiaa.org | DOI: 10.2514/2.5096

Table 5 Results of 3-DOF Monte Carlo simulations, 100 runs each

	Mission 1		Mission 2		Mission 3	
Parameter	Average	Standard deviation	Average	Standard deviation	Average	Standard deviation
Range, n mile	29.9	0.4	28.2	1.2	28.5	1.6
Heading, deg	−9.1	0.8	−3.3	6.6	−5.5	5.5
Altitude, ft	95,480	1006	97,959	1969	99,396	2472
Maximum heat rate, Btu · ft^2/s	67.7	1.6	69.4	1.7	66.9	1.4
Planner iterations	24.1	2.5	25.5	0.9	90.5	11.6
Update iterations	2.4	0.7	2.3	0.7	2.6	0.9

Table 6 Results of 3-DOF Monte Carlo simulations, 100 runs each

	Mission 4		Mission 5		Mission 6	
Parameter	Average	Standard deviation	Average	Standard deviation	Average	Standard deviation
Range, n mile	30.7	0.7	28.6	1.3	29.3	1.2
Heading, deg	7.7	4.2	−4.0	5.7	−7.0	3.4
Altitude, ft	99,372	1128	100,889	2177	99,252	1894
Maximum heat rate, Btu · ft^2/s	62.2	1.6	60.5	1.3	61.5	1.7
Planner iterations	19.9	1.4	23.2	1.2	22.6	0.6
Update iterations	2.5	0.6	2.4	0.7	2.3	0.5

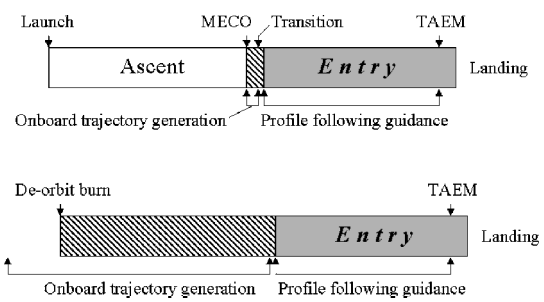

Fig. 7 Onboard trajectory generation execution scenarios for two mission types.

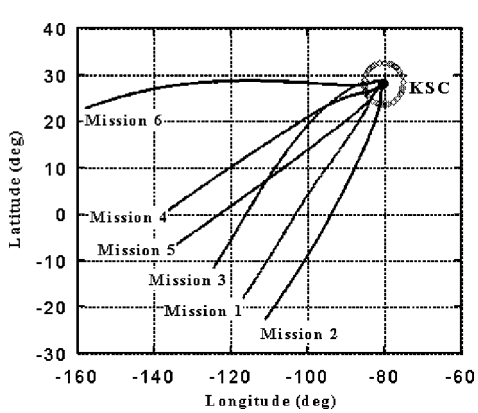

Fig. 8 Missions 1–6 ground tracks.

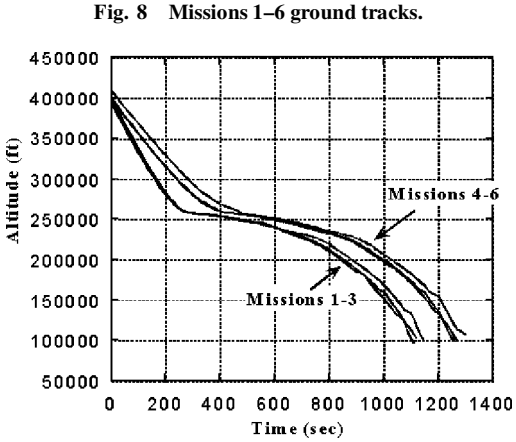

Fig. 9 Missions 1–6 altitude profiles.

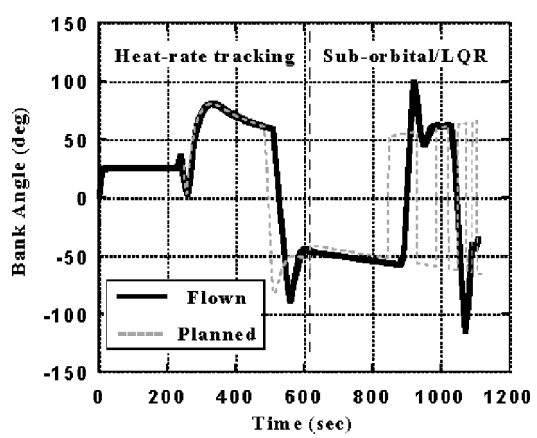

Fig. 10 Mission 1 bank angle profile.

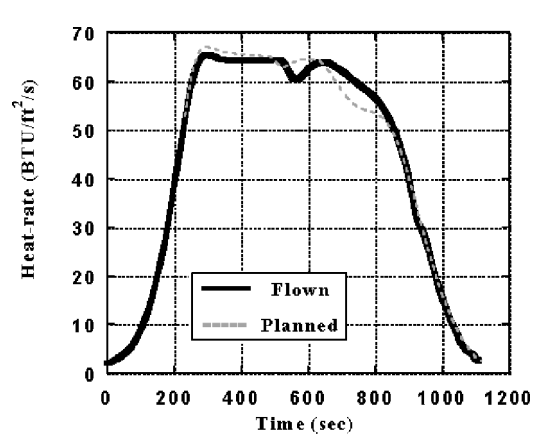

Fig. 11 Mission 1 heat-rate profile.

Summary

An automated method for computing orbital reentry trajectories with heating constraints was introduced. The algorithm based on this method, EGuide, was used successfully as guidance for a variety of suborbital and orbital entry missions. When an initial planning stage is incorporated to generate trajectories to be flown by a profile following guidance method and the scope of the entry problem is reduced to one that is fully characterized with four parameters, the issue of computational complexity is diminished. The unique setup of the orbital reentry problem provides additional benefits such as smooth control commands to the vehicle and a smooth altitude profile. The use of heat-rate tracking in the initial part of orbital

reentry is particularly effective for two reasons: First, it deals with the orbital reentry heating constraint directly through the use of feedback control. Second, the computationally efficient heat-rate tracking guidance allows for time to update (in predictor–corrector fashion) the parameters that shape the remainder of the trajectory.

References

[1]Harpold, J. C., and Graves, C. A., Jr., "Shuttle Entry Guidance," *Journal of the Astronautical Sciences*, Vol. 27, No. 3, 1979, pp. 239–267.

[2]Powell, R. W., "Numerical Roll Reversal Predictor–Corrector Aerocapture and Precision Landing Guidance Algorithms for the Mars Surveyor Program 2001 Missions," AIAA Paper 1998-4574, Aug. 1998.

[3]Spratlin, K. M., "An Adaptive Numeric Predictor–Corrector Guidance Algorithm for Atmospheric Entry Vehicles," M.S. Thesis, Dept. of Aeronautics and Astronautics, Massachusetts Inst. of Technology, Cambridge, MA, May 1987.

[4]Fuhry, D. P., "Adaptive Atmospheric Reentry Guidance for the Kistler K-1 Orbital Vehicle," *Proceedings of AIAA Guidance, Navigation, and Control Conference*, Vol. 2, AIAA, Reston, VA, 1999, pp. 1275–1288.

[5]Mease, K. D., Chen, D. T., Teufel, P., and Schoenenberger, H., "Reduced-Order Entry Trajectory Planning for Acceleration Guidance," *Journal of Guidance, Control, and Dynamics*, Vol. 25, No. 2, 2002, pp. 257–266.

[6]Shen, Z., and Lu, P., "Onboard Generation of Three-Dimensional Constrained Entry Trajectories," *Journal of Guidance, Control, and Dynamics*, Vol. 26, No. 1, 2003, pp. 111–121.

[7]Roenneke, A. J., "Adaptive Onboard Guidance for Entry Vehicles," AIAA Paper 2001-4048, Aug. 2001.

[8]Dukeman, G. A., "Profile Following Entry Guidance Using Linear Quadratic Regulator Theory," *Proceedings of AIAA Guidance, Navigation, and Control Conference*, Vol. 1, AIAA, Reston, VA, 2002, pp. 198–207.

[9]Press, W. H., Teukolsky, S. A., Vetterling, W. H., and Flannery, B. P., *Numerical Recipes in C*, 2nd ed., Cambridge Univ. Press, New York, 1993, pp. 379–389.

[10]Vinh, N. X., *Optimal Trajectories in Atmospheric Flight*, Elsevier, New York, 1981, pp. 47–62.

[11]Vinh, N. X., Busemann, A., and Culp, R. D., *Hypersonic and Planetary Entry Flight Mechanics*, Univ. of Michigan Press, Ann Arbor, MI, 1980, pp. 139–143.

[12]Justus, C. G., and Johnson, D. L., "The NASA/MSFC Global Reference Atmospheric Model: 1999 Version (GRAM-99)," NASA TM-209630, May 1999.

Downloaded by UNIVERSITY OF OKLAHOMA on January 28, 2015 | http://arc.aiaa.org | DOI: 10.2514/2.5096